

RADIAL SHRINKAGE OF SINGLE-WALLED CARBON NANOTUBE BUNDLES AT HIGH TEMPERATURES

YOSITAKA YOSIDA

Department of Material Science and Environmental Science, College of Science and Engineering, Iwaki Meisei University, Iwaki Fukushima 970-8551, Japan.

X-ray diffraction measurement on single-walled carbon nanotube (SWNT) bundles revealed radial shrinkage in the temperature range from 290 to 1600 K. The hysteretic temperature dependence was observed in the virgin run of cycling measurements. The result is discussed in terms of desorption of molecules from intertube space in the bundles and of a magnetic phase transition of ferromagnetic metal catalyst particles. In the second and third runs a simple temperature dependence was found. The linear expansivity as a function of temperature is determined by a linear-regression of the data between 290 and 330 K to be $(-1.52 \pm 0.05) \times 10^{-6} \text{ K}^{-1}$, and of the data between 1300 and 1550 K to be $(-2.48 \pm 0.05) \times 10^{-6} \text{ K}^{-1}$. The volume thermal expansion coefficient for the bundles is suggested to be negative over the measured temperature range by assuming that the tube-axis expansion is similar to the in-plane expansion for graphite.

1. Introduction

Single-walled carbon nanotubes (SWNTs) with diameter ranging from 0.6 to 6 nm [1-5] have been produced by a laser vaporization method [1] and a dc arc vaporization method [2, 4]. Both methods usually give entangled bundles (Fig. 1); SWNTs in a bundle have a closepacked two-dimensional (2D) arrangement with a lattice constant of $\sim 17 \text{ \AA}$ [1].

SWNTs can be constructed from monoatomic layer of graphite, i.e. 2D graphite, by connecting two equivalent lattice points with a chiral vector, $C=ma+nb=C(m, n)$, where m and n are integers, and a and b primitive translation vectors of 2D graphite. The modulus of a chiral vector therefore gives the circumference of a SWNT. The SWNTs with indices (m, m) , $(3m, 0)$, and $(3m, n)$ are called armchair tube, zigzag tube, and chiral tube, respectively. All of these tubes have been predicted to exhibit metallic electronic properties. The chiral tubes with indices other than $(3m, n)$ have been predicted to exhibit semiconductive or insulative electronic properties.

Many experimental studies [6-9] have supported to the predictions. A recent low-temperature scanning tunneling microscopy [10], however, shows that the finite curvature of SWNTs and intertube interactions now give implications for our understanding of the electronic properties and potential applications in nanoelectronic devices such as a field effect transistor [11], for example.

Terrones *et al.* [12] found coalescence of two tubes within a bundle under electron irradiation at high temperatures up to 1273 K; the bundle contained the coalesced tube throughout the process. They point out that coalescence seems to be restricted to tubes with the same chirality. Dillon *et al.* [13] explored an application of SWNTs bundles as a nanoporous system to hydrogen-storage material. Here, we show unexpected radial shrinkage of the bundles that is partially understood in

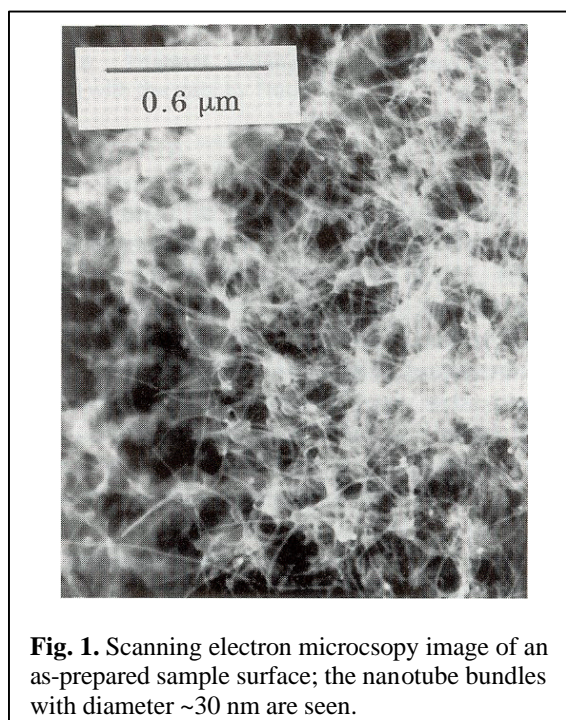


Fig. 1. Scanning electron microscopy image of an as-prepared sample surface; the nanotube bundles with diameter ~ 30 nm are seen.

terms of desorption of molecules from intertube space. Thus, intertube interactions seem to be an urgent subject to develop potential applications of SWNTs.

2. Experiment

X-ray diffraction (XRD) was carried out using a RINT-2000 (Rigaku) diffractometer attached a high temperature furnace. Copper anode was used as X-rays source. The sample was a pressed mat (~1 cm in diameter, ~0.05 cm in thickness) of the as-grown collar, and was directly put on a tungsten heater. XRD profiles were obtained at various fixed temperatures up to 1600 K in vacuum of 6×10^{-5} Pa. The sample temperature was determined by monitoring the (111) reflection of Ni which were dispersed throughout the as-grown mat; we referred to the published thermal expansion data [14].

To synthesize the SWNTs, a composite graphite anode containing a mixture of 1 at% Y, 4.2 at% Ni, and 94.8 at% C was prepared. A standard direct current (dc) arc experiment applying -40 V at 80 A under a partial helium pressure of 6.7×10^{-4} Pa was carried out. We found a soft black collar around the cathode deposit. The concentrations of impurities and of a variety of forms of carbon other than SWNTs were estimated by energy dispersive X-ray spectroscopy, differential temperature analysis, and thermogravimetric analysis. The results were reported elsewhere [15].

3. Results and Discussions

3-1. XRD Profile at 290 K

Thess *et al.* have reported XRD profile measured at 300 K for the SWNT bundles. The XRD profile is explained in terms of a two-dimensional arrangement of uniformly charged cylinders with a tube diameter of 13.80 Å and a van der Waals gap between cylinders of 3.15 Å; the SWNT form factor is approximated by the cylindrical Bessel function $J_0(QR)$, where R is the SWNT radius. $J_0(QR)$ modulates the positions and shapes of the peaks as well as their intensities.

In the present experiment, a profile of XRD measured at 290 K (Fig. 2(a)) shows five Bragg peaks up to $Q \sim 1.70 \text{ \AA}^{-1}$. Figure 2(b) shows the simulated profile and the XRD profile subtracted the background signals from Fig. 2(a). The vertical tick marks are Bragg positions in the infinite

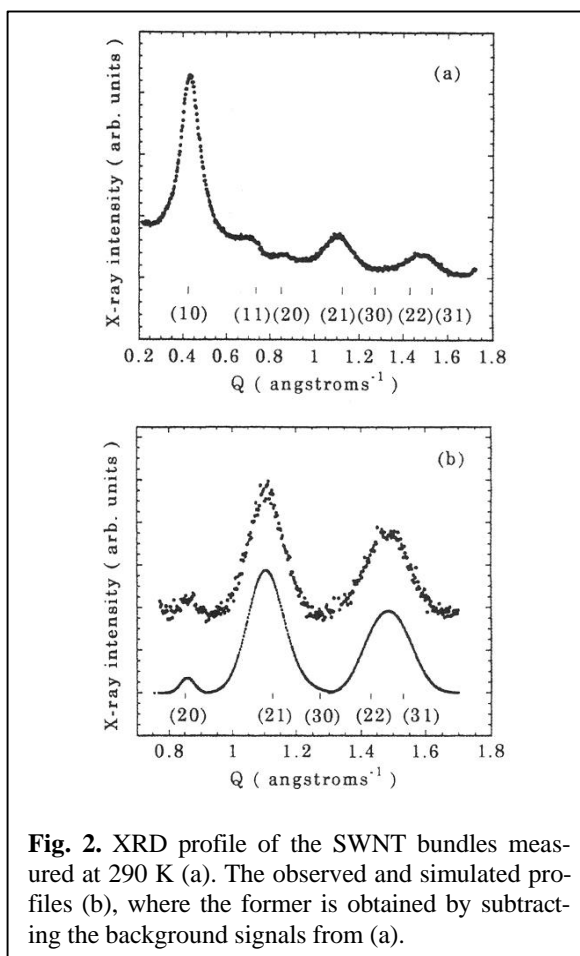


Fig. 2. XRD profile of the SWNT bundles measured at 290 K (a). The observed and simulated profiles (b), where the former is obtained by subtracting the background signals from (a).

crystal. The observed peak positions coincide with the calculated positions only when the calculated maxima for reflections happen to lie near peaks in $|J_0(QR)|$. In the simulation we assumed that the Bragg peaks were given by a Gaussian line shape. Thus, we derived the lattice constant $L_0 = 17.1 \pm 0.2 \text{ \AA}$ at 290 K for the 2D SWNT bundles. Our result of L_0 is in good agreement with the result of $16.9 \pm 0.2 \text{ \AA}$ reported by Thess *et al.*

3-2. Hysteresis of L_0 vs. T

L_0 as a function of T in the virgin run of three cycling measurements shows hysteretic behavior. Figure 3 shows a steep shrinkage from 17.1 Å at 290 K to 16.8 Å at ~650 K, and then a simple shrinkage to 16.7 Å at 1530 K. It shows a distinct kink at ~650 K. On cooling below 1600 K, it gradually expands to 16.9 Å at 290 K, somewhat smaller than an initial value of 17.1 Å.

There are three possible origins of the observed steep shrinkage and the related kink at 650

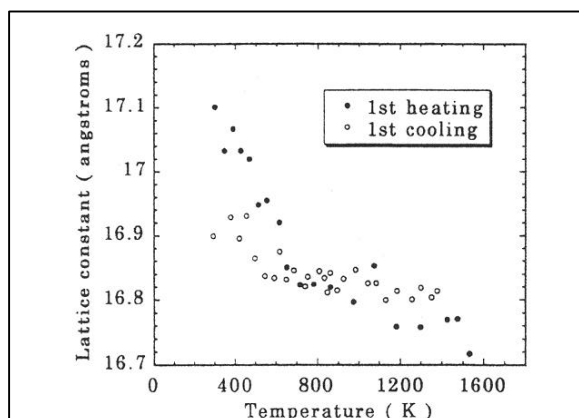


Fig. 3. L_0 vs. T plot of the SWNT bundles in the virgin run of three cycling measurements. A kink is found at about 650 K on heating; on cooling from 1600 K it seems to disappear. The difference of L_0 at 290 K can be explained by desorption of molecules from intertube space in the bundles. A magnetic phase transition of Ni particles from a ferromagnetic and a paramagnetic state at 631 K gives the most plausible explanation for the kink.

K; (1) a change of tube diameter from contraction to expansion with increasing T which is expected from in-plane expansion of graphite [16, 17], (2) desorption of molecules from the intertube space of bundles when the sample is heated under vacuum, and (3) a magnetic phase transition of Ni particles which are dispersed throughout the as-grown mat.

The distance between in-plane carbon atoms of graphite slightly contracts up to 673 K, and then turns to expand at high temperatures [16, 17]; the coefficient of expansion is $-1.0 \times 10^{-6} \text{ K}^{-1}$ at 300 K, 0 K^{-1} at 673 K, and $1.2 \times 10^{-6} \text{ K}^{-1}$ at 1500 K. Using this reported data, we estimated the magnitude of tube diameter shrinkage in the range from 300 K to 673 K to be only 0.2% of the observed steep shrinkage. We therefore excluded the possibility of tube diameter shrinkage.

We examined any possible role of desorption of molecules from the intertube space of bundles in the observed steep shrinkage; we put the sample in open air at 290 K after the three cycling measurements. We found $L_0=17.2 \text{ \AA}$ at 290 K, somewhat larger than the initial value of 17.1 \AA . This value remained unchanged in vacuum. When the sample was heated to 1600 K in vacuum, in this fourth run (not shown) we found the T -dependent L_0 quite similar to that in the first run, except for a constant upward shift by 0.1 \AA .

The result implies that the steep shrinkage observed below 650 K in the virgin and fourth runs results from an extrinsic origin; adhesion of molecules on the intertube space of bundles can cause the intertube distance to expand until an initial value particular for each bundle perfectly recovers; when heated the sample in vacuum desorption of molecules from the intertube space of bundles gives rise the observed steep shrinkage.

It is difficult to answer the question why the kink appears at $\sim 650 \text{ K}$ in terms of the desorption effect. This will be given by a magnetic phase transition of Ni particles, described later. Scanning electron microscopy has exhibited the entangled bundles (Fig. 1) as observed in previous studies [1, 2, 14]; they are more or less dense, depending on where they are deposited in the reactor. We found that high density entangled bundles contained large amount of Ni particles. The entangled bundles would require some forces to maintain their particular forms as observed. One could easily pullout some of these bundles from the mat by manipulating a ferromagnetic tip. This experiment suggests that the magnetic force is one of them. Similar experiment using a Pt tip has been made by Collins *et al.* [18], suggesting van der Waals force as another example. With increasing T above the Curie temperature of Ni, $T_c=631 \text{ K}$, the bundles will become free from this magnetic constraint. On cooling below T_c , their original constraint will never recover, because the bundles in the sample are loosely packed with a skeletal density of 0.606 g/cm^3 . These qualitatively explain the observed kink and hysteresis in the virgin and forth runs. A disappearance of the steep shrinkage in the second and third runs may support that the bundles are perfectly free from the magnetic constraint. Thus, the effect of the magnetic phase transition of Ni particles at 631 K can give rise the most plausible explanation for the temperature at which the kink is observed, and also the hysteretic behavior of L_0 .

3-3. Thermal Expansion of the SWNT Bundles

In the second and third runs (Fig. 4), it shows a simple behavior over the entire temperature range. We determined a relationship between L_0 and T by fitting the data obtained in these two runs: $L_0 (\text{\AA})=16.943 + 7.6459 \times 10^{-5}T - 1.864 \times 10^{-7}T^2 + 6.354 \times 10^{-11}T^3$ in the range 290-1600 K. We believe that the intrinsic lattice constant for

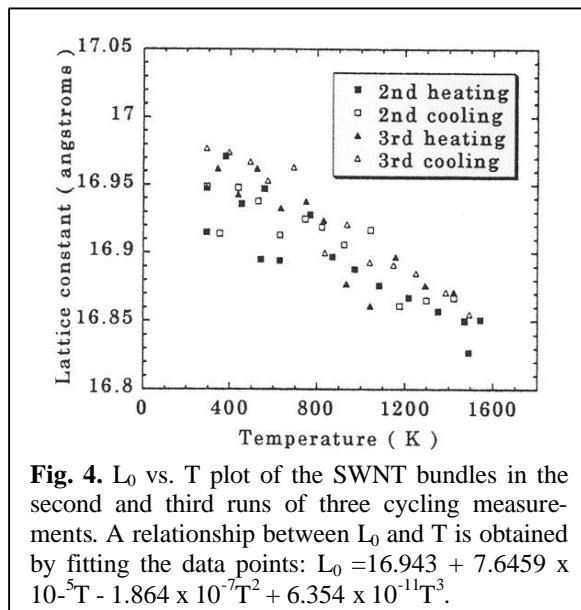


Fig. 4. L_0 vs. T plot of the SWNT bundles in the second and third runs of three cycling measurements. A relationship between L_0 and T is obtained by fitting the data points: $L_0 = 16.943 + 7.6459 \times 10^{-5}T - 1.864 \times 10^{-7}T^2 + 6.354 \times 10^{-11}T^3$.

SWNT bundles as a function of temperature is given by this relationship.

Figure 5 shows the T -dependent linear thermal expansivity $\Delta L_0/L_0(290)$ for the 2D SWNT lattice. The coefficient of linear expansion normal to the bundle axis, \mathbf{a}_\perp , was determined by a linear-regression analysis of the data between 290 K and 330 K to be $(-1.5 \pm 0.1) \times 10^{-6} \text{ K}^{-1}$. This value is by a factor of 10 smaller than those for solid C_{60} [19] and graphite [16, 17] in magnitude, and different in those sign. A similar analysis between 1300K and 1550K yields $\mathbf{a}_\perp = (-2.5 \pm 0.1) \times 10^{-6} \text{ K}^{-1}$. From the results of \mathbf{a}_\perp we can expect the negative coefficient of volume expansion, $\alpha_v = \alpha_\parallel + 2 \mathbf{a}_\perp$ in the SWNT bundles over the measured temperature range, if we assume that the thermal expansion along the bundle axis, α_\parallel , is given by that along the fiber axis in vapor-grown carbon fibers [20] $[(1.2-1.8) \times 10^{-6} \text{ K}^{-1}$ at about 1500 K] or that along the a axis in graphite $(\sim 1.2 \times 10^{-6} \text{ K}^{-1}$ at 1500K), as pointed out by Ruoff and Lorents [21] and Ebbesen [20]. The assumption is also supported by simulations [22, 23] showing that the strength of the in-plane chemical bond is similar for graphite plane and for a SWNT.

The negative volume expansivity is best approached by a consideration of the Gruneisen factor [24]. From statistical mechanics a volume expansivity can be derived,

$$\Delta V/V = -\kappa k_B T V \sum \ln v_j / \ln V = \kappa_B T V \sum \gamma_j,$$

$$\Sigma \gamma_j = -\Sigma \ln v_j / \ln V,$$

where κ is the compressibility, γ_j the Gruneisen factor for each vibrational frequency, and V the

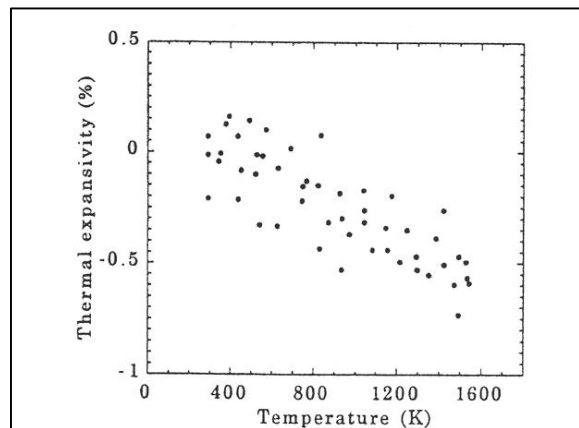


Fig. 5. Isobaric linear expansivity $\Delta L_0/L_0(290)$ vs. T for the 2D SWNT Lattice; $L_0(290) = 17.1 \pm 0.2 \text{ \AA}$. The data points are obtained from the second and third runs as shown in Fig. 4.

volume per gram atom. Since κ for a SWNT bundle is positive [25], we can obtain that $\Sigma \gamma_j$ is negative. This implies that the frequency of lattice vibration decreases with decreasing volume. Phonon dispersion relations for the 2D SWNT lattice will give a physical interpretation of this negative $\Sigma \gamma_j$; for solids with the ZnS type structure, for example, Blackman [26] theoretically has shown that $\Sigma \gamma_j$ for the transverse mode is negative and dominates the longitudinal mode.

4. Conclusion

We determined the 2D lattice constant L_0 of the SWNTs in the bundles by X-ray diffraction in the temperature range from 290 K to 1600 K. The simulation of XRD profile using a Gaussian line shape for each Bragg peak gave $L_0 = 17.1 \pm 0.2 \text{ \AA}$ at 290 K. It shrank over the entire temperature range. A kink of L_0 at about 650 K found in the virgin run is successfully explained by a magnetic phase transition of Ni particles between a ferromagnetic and a paramagnetic state at 631 K. The steep shrinkage observed below 650 K in the virgin run can be understood in terms of desorption of molecules from the intertube space of the bundles. Based on the data obtained from the successive runs, we determined the intrinsic lattice constant as a function of temperature. We also found that the isobaric linear thermal expansion coefficient normal to the bundle axis was negative over the entire temperature range.

Acknowledgment

This work was performed using facilities of High Technique Research Center, Iwaki Meisei University.

REFERENCES

- [1] A. Thess, R. Lee, P. Nikolaev, H. Dai, P. Petit, J. Robert, C. Xu, Y. H. Lee, S. G. Kim, A. G. Rinzler, D. T. Colbert, G. E. Scuseria, D. Domanek, J. E. Fischer, and R. E. Smalley, *Science* **273**, 483 (1996).
- [2] C. Journet, W. K. Maser, P. Bernier, A. Loiseau, M. Lamy de Chapel Ie, S. Lefrant, P. Deniard, R. Lee, and J. E. Fischer, *Nature (London)* **388**, 756 (1997).
- [3] H. Dai, A. G. Rinzler, P. Nikolaev, A. Thess, D. T. Colbert, and R. E. Smalley, *Chem. Phys. Lett.* **269**, 471 (1996).
- [4] Y. Yosida, S. Shida, T. Ohsuna, and N. Shiraga, *J. Appl. Phys.* **76**, 4533 (1994).
- [5] C-H. Kiang, W. A. Goddard III, R. Beyers, and D. S. Bethune, *Carbon* **33**, 903 (1995).
- [6] M. Bockrath, D. H. Cobden, P. L. McEuen, N. G. Chopra, A. Zetti, A. Thess, R. E. Smalley, *Science* **275**, 1992 (1997).
- [7] S. J. Tans, M. H. Devoret, H. Dai, A. Thess, R. E. Smalley, L. J. Geerligs, C. Dekker, *Nature (London)* **386**, 474 (1997).
- [8] J. W. G. Wildoer, L. C. Venema, A. G. Rinzler, R. E. Smalley, C. Dekker, *Nature (London)* **391**, 59 (1998).
- [9] T. W. Odorn, J-L. Huang, P. Kim, C. M. Lieber, *Nature (London)* **391**, 62 (1998).
- [10] M. Ouyang, Jin-Lin Huang, C. Li, Cheung, C. M. Lieber, *Science* **292**, 702 (2001).
- [11] S. J. Tans, A. R. M. Verschueren, C. Dekker, *Nature (London)* **393**, 49 (1998).
- [12] M. Terrones, H. Terrones, F. Banhart, J.-C. Charlier, P. M. Ajayan, *Science* **288**, 1226 (2000).
- [13] A. C. Dillon, K. M. Jones, T. A. Bekkedahl, C. H. Kiang, D. S. Bethune, M. J. Heben, *Nature (London)* **386**, 377 (1997).
- [14] Thermal Expansion/Metallic Element and Alloys, in *Thermophysical Properties of Matters*, The TPRC Data Series Vol. 12, edited by Y. S. Touloukian, R. K. Kirby, R. E. Taylor, and P. D. Desai (Plenum, New York, 1975), p.226.
- [15] Y. Yosida and I. Oguro, *J. Appl. Phys.* **86**, 999 (1999).
- [16] E. G. Steward, B. P. Cook, and E. A. Keller, *Nature (London)* **187**, 1015(1960).
- [17] W. C. Morgan, *Carbon* **10**, 73 (1972).
- [18] P. G. Collins, A. Zettl, H. Bando, A. Thess, R. E. Smalley, *Science* **278**, 100 (1997).
- [19] P. A. Heiney, G. B. M. Vaughan, J. E. Fischer, N. Coustel, D. E. Cox, J. R. D. Copley, D. A. Neuman, W. A. Kamitakahara, K. M. Greegan, D. M. Cox, J. P. McCauley, Jr., A. B. Smith III, *Phys. Rev.* **B45**, 4544 (1992).
- [20] Carbon nanotubes, Preparation and Properties, edited by T. W. Ebbesen (Chemical Rubber, Boca Raton, FL, 1997), p. 96.
- [21] R. S. Ruoff and D. C. Lorentz, *Carbon* **33**, 925 (1995).
- [22] J. P. Lu, *Phys. Rev. Lett.* **79**, 1297 (1997).
- [23] E. Hernandez, C. Goze, P. Brenier, A. Rubio, *Phys. Rev. Lett.* **80**, 4502 (1998).
- [24] T. H. K. Barron, J. G. Collins, G. K. White, *Adv. Phys.* **29**, 609 (1980).
- [25] J-P. Salvetat, G. A. D. Briggs, J-M. Bonard, R. R. Basca, A. J. Kulik, T. Stockli, N. A. Burnham, L. Forro, *Phys. Rev. Lett.* **82**, 944 (1999).
- [26] M. Blackman, *Philo. Mag.* **3**, 831 (1958).